Asian Journal of Chemistry; Vol. 24, No. 3 (2012), 1135-1140

ASIAN JOURNAL OF CHEMISTRY

www.asianjournalofchemistry.co.in

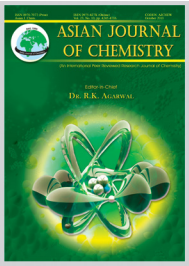

Synthesis, Characterization and Photocatalytic Activity of Anatase-Brookite-Rutile Composite TiO_2 Nanocrystals Prepared in H_2O/Alcohol System

S.Z. HU*, F.Y. LI and Z.P. FAN

Institute of Eco-environmental Sciences, Liaoning Shihua University, Fushun 113001, P.R. China

*Corresponding author: Tel: +86 24 23847473; E-mail: hushaozheng001@163.com

(*Received*: 18 February 2011; *Accepted*: 9 November 2011) AJC-10610

Anatase-brookite-rutile composite TiO_2 nanocrystals with a narrow particle size distribution and good dispersibility were prepared by a hydrothermal method using $TiC1_4$ as the starting material in different H_2O/alcohol system. TEM, HRTEM, X-ray diffraction, UV-VIS diffuse reflectance spectra and FT-IR were used to characterize the synthesized particles. The results showed that the presence of alcohol was the key factor which determined the phase content in prepared TiO_2. The prepared TiO_2 exhibited higher photocatalytic activity than P25 under UV light.

Key Words: Anatase-brookite-rutile composite TiO_2, H_2O/alcohol system, Photocatalysis, Phase ratio.

INTRODUCTION

The preparation of nano-sized TiO_2 has attracted much attention due to its excellent dielectric property, optical property, gas-sensing behaviour and photocatalytic property[1,2]. As a popular photocatalyst, TiO_2 has been widely studied because of its various merits, such as optical-electronic properties, low-cost, chemical stability and non-toxicity. Nano-sized TiO_2 can be synthesized by several methods. Among them, the hydrothermal synthesis, which is called "soft solution chemical processing", is one of the most commonly used methods[3-5].

The photocataltsis behaviour is initiated by the surface trapping of photoinduced electron-hole pairs, including interfacial charge transfer reactions with the target pollutant molecules, resulting in their complete degradation[6] to CO_2. The current bottleneck in photocatalysis lies in its low quantum yield, which depends on the ratio of the surface charge carrier transfer rate to the electron-hole recombination rate.

To increase the quantum yield of nanocrystalline photocatalysts, the electron-hole recombination has to be reduced. A number of research groups have approached this problem by many methods. Zhang *et al.*[7], reported that the particle size played an important role in photocatalytic reaction. With a smaller particle size, the number of active surface sites increased and so did the surface charge carrier transfer rate in photocatalysis. Therefore, the electron-hole recombination was reduced. On the other hand, the smaller particle size caused the larger BET which could absorb more hydroxyl group. Photogenerated holes were trapped by surface hydroxyl group, producing active surface hydroxyl radicals, which played crucial roles in photocatalytic reactions[8]. Miyauchi *et al.*[9], reported that the surface modification of TiO_2 led to the charge transfer between the TiO_2 and modified layers which reduced the recombination. Li *et al.*[10] reported that doping with transition metal ions into TiO_2 lattice could reduce the recombination of electron-hole pairs significantly. Ohno *et al.*[11] reported that the synergistic effect between anatase and rutile phase allowed the migration of photogenerated electrons from anatase phase to rutile phase and retarded the recombination of the electrons and holes in anatase. Ozawa *et al.*[12] reported that anatase-brookite composite nanocrystals exhibited a higher activity for the gas-phase oxidation of CH_3CHO than pure anatase nanocrystal which resulted from the increase in charge separation efficiency.

It has been reported that the anatase-brookite and anatase-rutile composite nanocrystals showed the better photocatalytic activity than pure anatase. However, little investigation on the photocatalytic activity of anatase-brookite-rutile composite TiO_2 nanocrystals was reported. In order to investigate the effect of the phase ratio of TiO_2 on photocatalytic efficiency, the most important precondition is to prepare all TiO_2 catalysts with comparable particle size which plays a significant role in photocatalytic activity. However, the particle size was always changed when altered the phase ratio of TiO_2. In present studies, the anatase-brookite-rutile composite TiO_2 nanocrystals with different phase ratio and comparable particle size were synthesized in H_2O/alcohol system. The photocatalytic performance

of the prepared nano-sized TiO_2 was tested in the degradation of methylene blue in water.

EXPERIMENTAL

Preparation and characterization: 0.8 mL $TiCl_4$ was added dropwise into Y mL methanol, ethanol and isopropanol to form solution A, respectively. 0.015 g PEG-4000 and 0.2 g urea were dissolved in (30-Y) mL de-ionized water to obtain solution B. Then the solution A was mixed with solution B under stirring for 10 min. The mixture was transferred into a 30 mL Teflon-lined autoclave, which was heated at 120 ºC for 6 h. After hydrothermal reaction, the solid product was washed with ethanol for three times and separated by centrifugation. The white TiO_2 precipitate was dried under vacuum overnight at room temperature and denoted as TCX-Y, where X and Y stands for the number of carbon in alcohol and the volume of alcohol, respectively.

XRD patterns were recorded on a Rigaku D/max-2400 instrument using CuK_α radiation (λ = 1.54 Å). The data were collected for scattering angles ranging between 20 and 70º, with a step of 0.02º. TEM and HRTEM image was measured by using a Philips Tecnai G220 electron microscope at an accelerating voltage of 200 kV. Fourier transform infrared spectra (FT-IR) were obtained on a Nicolet 20DXB FT-IR spectrometer. UV-VIS spectroscopy measurement were carried out with a GASCO V-550 model UV-VIS spectrophotometer, using $BaSO_4$ as the reflectance sample.

Photocatalytic experiment: The photocatalytic performance of samples was tested in the degradation of the methylene blue in aqueous medium. 25 mg TiO_2 nanoparticles were dispersed in 100 mL aqueous solution of methylene blue (50 ppm) in an ultrasound generator for 10 min. The suspension was transferred into a 150 mL beaker with water-cooled cylindrical jacket and then under stirring for 0.5 h in darkness to achieve adsorption-desorption equilibrium. Then the suspension was exposed to a 125 W high-pressure mercury lamp in a water-cooled cylindrical jacket and air was bubbled through the suspension under stirring. At given time intervals, 4 mL suspension was taken and immediately centrifuged for 20 min. All runs were conducted at ambient pressure and 30 ºC. For comparison, a commercial catalyst Degussa P25 was used.

The concentration of methylene blue was measured by a UV-visible spectrophotometer at 665 nm. The percentage degradation was determined as follows:

$$D\,(\%) = \frac{A_0 - A}{A_0} \times 100$$

where A_0 and A are the absorbances of the liquid samples before and after degradation, respectively.

RESULTS AND DISCUSSION

The XRD patterns of the prepared TiO_2 particles were illustrated in Fig. 1. The particle sizes of the catalysts were calculated by their XRD patterns according to the Debye-Scherrer equation[13]. The phase contents of the samples can be estimated from their respective XRD peak intensities using the method of Zhang and Banfield[14]:

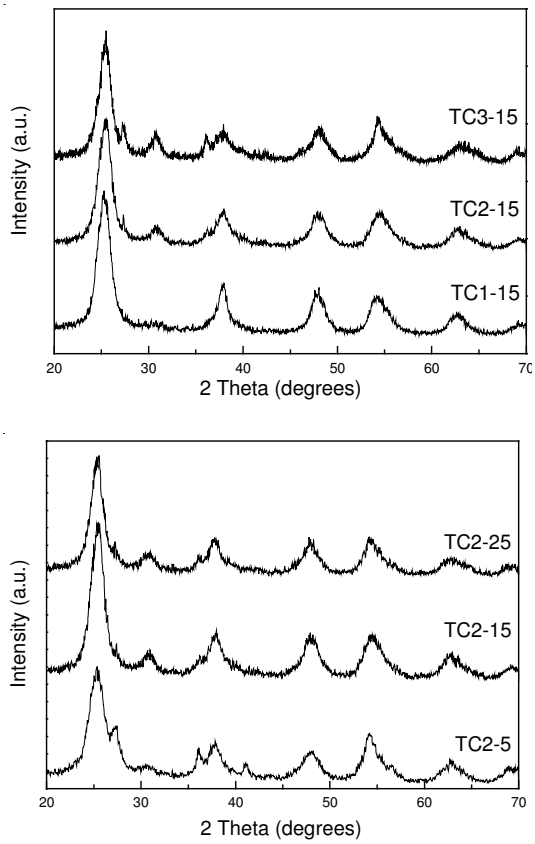

Fig. 1. XRD patterns of the prepared TiO_2 powders

$$X_A = \frac{k_A I_A}{(k_A I_A + I_R + k_B I_B)} \quad (1)$$

$$X_B = \frac{k_B I_B}{(k_A I_A + I_R + k_B I_B)} \quad (2)$$

$$X_R = \frac{I_R}{(k_A I_A + I_R + k_B I_B)} \quad (3)$$

where X_A, X_B and X_R represent the weight fraction of anatase, brookite and rutile, respectively. I_A, I_B and I_R are the intensities of the anatase (101), brookite (121) and rutile (110) diffraction peaks, respectively. The phase identification and approximate crystallite size of the TiO_2 from XRD analysis were summarized in Table-1. It was indicated that the prepared samples were anatase-brookite-rutile composite nanocrystals. The anatase (rutile) content decreased (increased) when adding methanol, ethanol and isopropanol in turn. The anatase (rutile) content increased (decreased) firstly and then decreased (increased) when adding the amount of ethanol from 5-15 mL and finally 25 mL. The possible reason will be discussed later. In addition, the prepared samples with different anatase-brookite-rutile phase ratio owned almost the same particle size around 5 nm.

Fig. 2 shows the TEM and HRTEM micrographs of the prepared TiO_2 particles and P25. Fig. 2A-E indicate that the prepared TiO_2 particles own almost the same particle size around 5 nm which are consistent with those calculated results from the XRD analysis (Table-1). Moreover, the prepared TiO_2 particles also exhibit narrow particle size distribution and

TABLE-1
PHASE RATIO, PARTICLE SIZE AND D (%) OF PREPARED TiO_2 COMPOSITE NANOCRYSTALS

Sample	$X_A/X_B/X_R$ (%)	Size (nm)	D (%)
TC2-5	51/20.5/28.5	5.0	81.2
TC2-15	59.9/27.2/12.9	4.8	99.5
TC2-25	55.8/28.6/15.6	5.3	96.5
TC1-15	100/0/0	5.0	93.2
TC3-15	50.6/31.6/17.7	5.2	90.9
P25	76/0/24	29.0	85.8

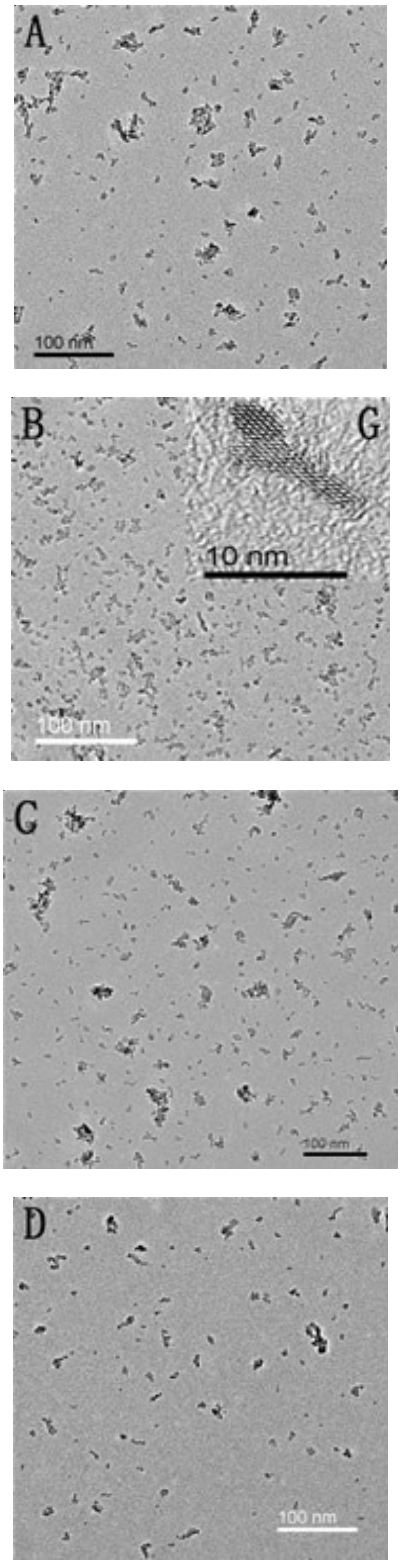

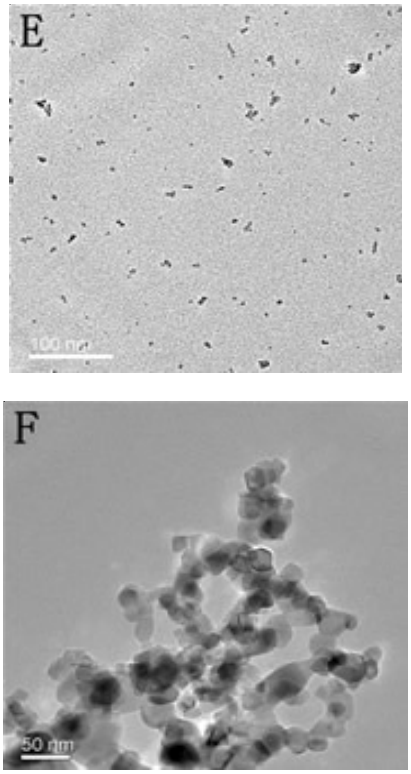

Fig. 2. TEM micrographs of TC1-15 (A), TC2-15 (B), TC3-15 (C), TC2-5 (D), TC2-25 (E), P25 (F) and HRTEM of TC2-15 (G)

good dispersibility. As shown in Fig. 2G, the HRTEM of TC2-25 shows that the prepared particles had a good crystalline structure. In Fig. 2F, the particle size of P25 is about 25-50 nm, which is much bigger than prepared TiO_2 particles (Fig. 2A-E). Moreover, the particles of P25 exhibited a poor dispersibility.

In order to elucidate the role of ethanol in the synthesis process, the hydrothermal reaction was terminated after 1 h by cooling the autoclave in running water. The solid in suspension was separated by centrifugation. The FT-IR spectrum of the obtained liquid sample was measured and shown in Fig. 3. The bands at 1630 and 3400 cm^{-1} were attributed to the bending and stretching vibrations of hydroxyl group, respectively. The bands around 2900-2800 cm^{-1}, 1380 and 1460 cm^{-1} were attributed to stretching and bending vibrations of C-H, respectively. The band around 870-810 cm^{-1} was attributed to C-C vibration. The band at 1020 cm^{-1} could be assigned to C-O stretching vibration of alcohol. The band at 1100 cm^{-1} could be assigned to Ti-O-C group vibration which indicated that the alcohol reacted to $TiCl_4$ and formed Ti-O-C group before hydrolysis process began[15]. In addition, it is noticed that the intensity ratio of Ti-O-C band to C-O band increased in sequence of TC1-15 < TC2-15 < TC3-15. This indicated that the hydrolysis velocity of Ti-O-R decreased in sequence of TC1-15 > TC2-15 > TC3-15. The possible reason will be explained in detail latter.

The UV-VIS diffuse reflectance spectra of prepared samples were presented in Fig. 4. The sequence of absorbing band edge of prepared samples was consistent with the anatase content in prepared TiO_2 which resulted from XRD. The band gaps of the TiO_2 samples were calculated according the method of Oregan *et al.*[16]. The result showed that the band gaps of

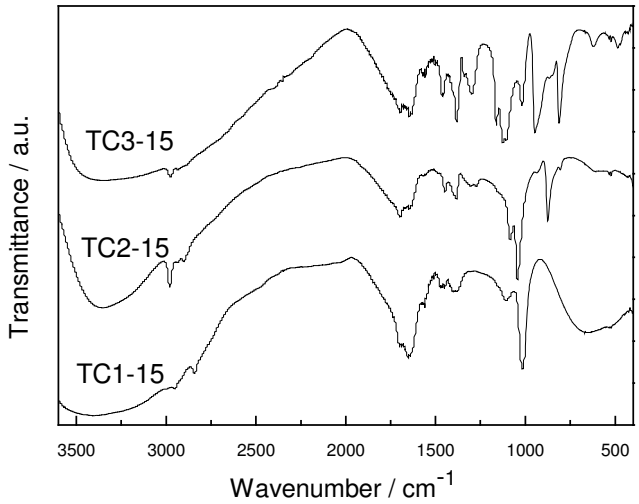

Fig. 3. FT-IR spectra of the obtained liquid samples

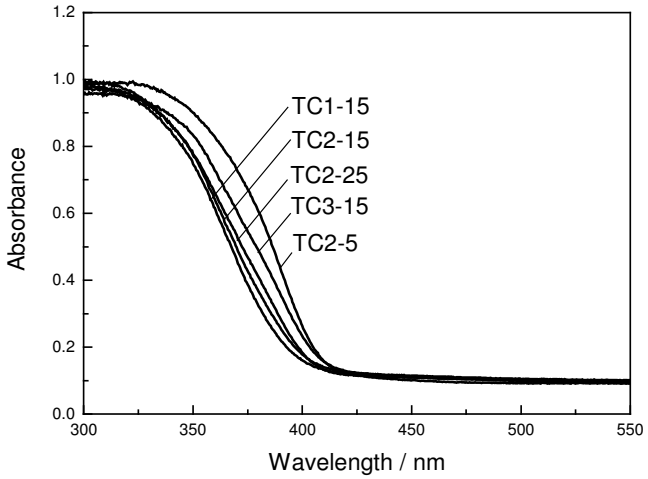

Fig. 4. UV-VIS diffuse reflectance spectra of prepared samples

TC2-5, TC2-15, TC2-25, TC1-15 and TC3-15 were 3.02, 3.04, 3.08, 3.08 and 3.02 eV. In addition, the UV-VIS absorption band edge was a strong function of TiO_2 size for diameters less than 10 nm, which can be attributed to the well-known quantum size effect for semiconductors. Such quantum size effect could enhance the redox ability of photogenerated e^+/h^- which is beneficial to the photocatalytic performance[17].

$$Ti-Cl+ROH \longrightarrow Ti-O-R+HCl \quad \text{Esterification} \qquad (4)$$

$$Ti-O-R+H_2O \longrightarrow Ti-OH+ROH \quad \text{Hydrolysis} \qquad (5)$$

$$Ti-OH+Ti-O-R \longrightarrow Ti-O-Ti+ROH \quad \text{Oxolation} \qquad (6)$$

$$Ti-OH+Ti-OH \longrightarrow Ti-(OH)_2-Ti \quad \text{Olation} \qquad (7)$$

Zhang *et al.*[14], reported that the transformation between anatase and brookite was reversible at lower temperatures (below 623 K). Moreover, little report on the formation mechanism of brookite is reported so far. Therefore, we considered brookite and anatase as a whole for predigestion of formation mechanism. According to the reaction process proposed by Gao *et al.*[18] and Chemseddine and Moritz[19], the possible reaction process may be as follows. In the presence of alcohol, $TiC1_4$ reacts readily with alcohol to form Ti-O-R and HCl which has been proved by FT-IR [eqn. 4]. Ti-O-R hydrolyzes to form Ti-OH and ROH [eqn. 5]. Then Ti-OH condense with Ti-O-R or Ti-OH to form Ti-O-Ti or Ti-$(OH)_2$-Ti structure [eqns. 6 and 7]. If an olation pathway dominates the condensation process, condensation can proceed along apical directions, leading to the skewed chains of the anatase structure. Otherwise, oxolation pathway dominates the condensation process which leading to the rutile structure[20,21]. Therefore, the anatase content in TiO_2 mainly lies on the reaction velocity of hydrolysis process. The faster hydrolysis velocity will lead to the generation of more hydroxyl group, which are favorable for olation and result in more anatase content in TiO_2. By contraries, hydrolysis reaction is incomplete and more rutile will be formed[18]. It is widely accepted that a stronger nucleophilic substitution reaction between H_2O and alkoxide molecules will occur when hydrolysis reaction of Ti-O-R happen and alkoxyl group in the alkoxide will be substituted by hydroxyl groups[22] of H_2O. According to that, the possible hydrolysis process of Ti-O-R [eqn. 5] is shown in **Scheme-I**. The whole process is divided into four steps. Step 1, Ti-O bond of Ti-O-R was weakened when O atom of H_2O lay aboard Ti atom. Step 2, Ti-O broke, Ti^+ and $[OR]^-$ were formed. Step 3, Ti^+ bond with O atom of H_2O and then positive charge of Ti^+ transferred to O atom which caused the weakness of one O-H bond in H_2O. Step 4, the O-H bond, which was weakened, broke and Ti-OH was formed. At the same time, H^+ bond with $[OR]^-$ to form R-OH. Therefore, the reaction velocity of this hydrolysis process mainly lies on the stability of $[OR]^-$. The better stability of $[OR]^-$ causes the faster hydrolysis velocity. The electron donation ability of alkyl group follows the order: $-CH_3 < -C_2H_5 < -CH(CH_3)_2$, which causes the stability sequence of $[OR]^-$ is $[OCH_3]^- > [OC_2H_5]^- > [OCH(CH_3)_2]^-$. So the Ti-O-R hydrolysis velocity follows the order: Ti-O-CH_3 > Ti-O-C_2H_5 > Ti-O-$CH(CH_3)_2$. Based on the above results, the sequence of anatase content in samples follows the order: TC1-15 > TC2-15 > TC3-15.

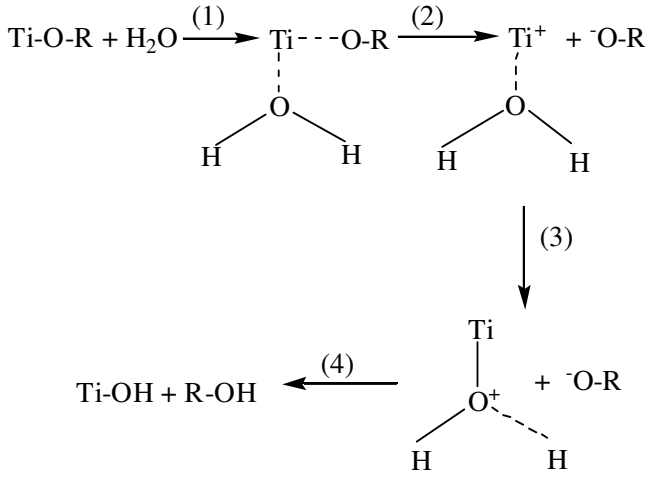

Scheme-I: Hydrolysis reaction mechanism of Ti-O-R

As for the different anatase content in TC2-5, TC2-15 and TC2-25, the possible reason may be as follows. When pure H_2O was used instead of H_2O/ethanol system, the prepared TiO_2 was the mixtures phases of anatase (49.5 %)

and rutile (50.5 %)[23]. Whereas, the phase content of TC2-5 was XA/XB/XR = 51 %/20.5 %/28.5 %. Based on the above results, the addition of ethanol increased the hydrolysis velocity which might be attributed to the decrease of system polarity. When the amount of ethanol was increased to 15 mL, this trend went on working. However, when 25 mL ethanol was used, the amount of H_2O decreased dramatically and Ti/H_2O ratio increased sharply which caused the hydrolysis of Ti-OC_2H_5 was incomplete[18]. Therefore, the anatase (rutile) content was increased (decreased) firstly and then decreased (increased) when adding the amount of ethanol from 5-15 mL and finally 25 mL.

Fig. 5 showed the photocatalytic activities of different samples. All the prepared samples except TC2-5 showed higher photocatalytic activity than P25 under UV light. This might be attributed to several reasons. First of all, the small particle size of photocatalyst accelerated the surface charge carrier transfer which decreased the chance of the recombination of the photoinduced electron-hole pairs, hence increasing the photocatalytic activity[7]. Secondly, the small particle size caused the large BET which could absorb more hydroxyl group, which were considered to play a key role in the photocatalytic reaction because the photoinduced holes could attack those surface hydroxyl groups and yield surface hydroxyl radicals with high oxidation capability[8]. Thirdly, the quantum size effect which was exhibited by prepared TiO_2 enhanced the redox ability of photogenerated e^+/h^- [17,24].

Ding *et al.*[25], reported that anatase was the active phase in photocatalytic reactions. Pure rutile normally showed no activity at all. Some other reports suggested that pure rutile did have some activity, but its performance was dependent on the preparation procedure of the photocatalyst and the nature of the precursor compound and the organic reactant[26,27]. However, the mixtures of anatase and rutile usually show higher photocatalytic activity than the pure anatase[11]. The reason may be that the energy band of anatase and rutile is 3.2 and 3.0 eV, respectively. In the photocatalysis reaction, the photogenereted electrons are accelerated to aggregate on anatase phase whereas the photogenereted holes to aggregate on rutile phase at the same time[11]. This synergetic effect between anatase and rutile may reduce the recombination of photogenerated electrons and holes significantly and lead to the better photocatalytic activity than pure anatase TiO_2. As for the anatase-brookite composite nanocrystals, the high activity resulted from interfacial electron transfer *via* the junction between anatase and brookite nanocrystals[12]. Thus it is easy to understand that the anatase-brookite-rutile composite nanocrystals with a befitting phase ratio may also exhibit high photocatalytic activity. Table-1 indicated that TC2-15 ($X_A/X_B/X_R$ = 59.9 %/27.2 %/12.9 %) and TC2-25 ($X_A/X_B/X_R$ = 55.8 %/28.6 %/15.6 %) showed better photocatalytic activity than other samples including pure anatase (TC1-15). The prepared TiO_2 nanoparticles with different phase ratio owned the almost same particle size (Table-1). So the influence of particle size on photocatalytic activity could be ignored. Therefore, these high activities may be attributed to the befitting anatase/brookite ratio around 2:1 which was consistent with the result of Ozawa *et al.*[12]. TC2-15 showed better activity than TC2-25 may be attributed to the more befitting anatase/rutile ratio (around 4.6:1). In addition, the photocatalytic activity of P25 ($X_A/X_B/X_R$ = 76 %/0/24 %) was higher than TC2-5 ($X_A/X_B/X_R$ = 51 %/20.5 %/28.5 %) even if the particle size of TC2-5 (*ca.* 5 nm) was much smaller than P25 (*ca.* 29 nm). This fact confirmed that the phase ratio of TiO_2 played as an important role as particle size in photocatalytic activity.

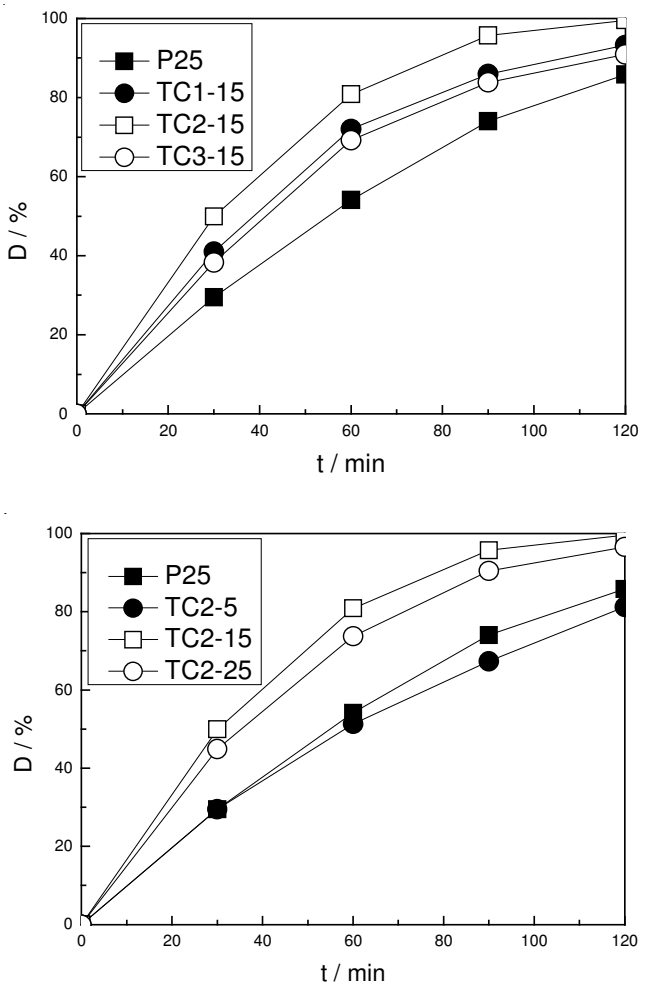

Fig. 5. Percentage degradation of the methylene blue in aqueous solution under UV light as a function of reaction time

Conclusion

Anatase-brookite-rutile composite TiO_2 nanocrystals with a narrow particle size distribution and good dispersion were prepared by a hydrothermal method. The results showed that the presence of alcohol was the key factor which determines the phase content in TiO_2. The anatase (rutile) content was decreased (increased) when adding methanol, ethanol and isopropanol in turn. The anatase (rutile) content was increased (decreased) firstly and then decreased (increased) when adding the amount of ethanol from 5-15 mL and finally 25 mL. The possible reaction mechanism was nucleophilic substitution reaction between H_2O and Ti-O-C band. The better stability of $[OR]^-$ causes the faster hydrolysis velocity, leading more anatase formed. The photocatalytic activity of the prepared samples was higher than P25 under UV light. The prepared anatase-brookite-rutile composite TiO_2 nanocrystals showed higher photocatalytic activity than pure anatase TiO_2. The phase

ratio of TiO_2 played as an important role as particle size in photocatalytic activity.

ACKNOWLEDGEMENTS

This work was supported by National Natural Science Foundation of China (No. 41071317, 30972418), National Key Technology R & D Programme of China (No. 2007BAC16B07), the Natural Science Foundation of Liaoning Province (No. 20092080). The authors would like to thank Prof. Anjie Wang, Dalian University of Technology, for the contribution to the manuscript.

REFERENCES

1. A.M. Djerdjev, J.K. Beattie and R.W. O'Brien, *Chem. Mater*., **17**, 3844 (2005).
2. J. Wang, S. Uma and K.J. Klabunde, *Appl. Catal. B*, **48**, 151 (2004).
3. J. Nian and H. Teng, *J. Phys. Chem. B*, **110**, 4193 (2006).
4. M. Wu, G. Lin, D. Chen, G. Wang, D. He, S. Feng and R. Xu, *Chem. Mater*., **14**, 1974 (2002).
5. H. Cheng, J. Ma, Z. Zhao and L. Qi, *Chem. Mater*., **7**, 663 (1995).
6. M.R. Hoffman, S.T. Martin, W.Y. Choi and D.W. Bahnemann, *Chem. Rev*., **95**, 69 (1995).
7. Z.B. Zhang, C.C. Wang, R. Zakaria and J.Y. Ying, *J. Phys. Chem. B*, **102**, 10871 (1998).
8. Q.J. Yang, C. Xie, Z.L. Xu, Z.M. Gao and Y.G. Du, *J. Phys. Chem. B*, **109**, 5554 (2005).
9. M. Miyauchi, A. Nakajima, K. Hashimoto and T. Watanabe, *Adv. Mater*., **12**, 1923 (2000).
10. F.B. Li, X.Z. Li, M.F. Hou, K.W. Cheah and W.C.H. Choy, *Appl. Catal. A*, **285**, 181 (2005).
11. T. Ohno, K. Tokieda, S. Higashida and M. Matsumura, *Appl. Catal. A*, **244**, 383 (2003).
12. T. Ozawa, M. Iwasaki, H. Tada, T. Akita and K. Tanaka, *J. Colloid Interf. Sci*., **281**, 510 (2005).
13. J. Lin, Y. Lin, P. Liu, M.J. Meziani, L. F. Allard and Y.P. Sun, *J. Am. Chem. Soc*., **124**, 11514 (2002).
14. H.Z. Zhang and J.F. Banfield, *J. Phys. Chem. B*, **104**, 3481 (2000).
15. D. Wang, R. Yu, N. Kumada and N. Kinomura, *Chem. Mater*., **11**, 2008 (1999).
16. B. O'Regan and M. Gratzel, *Nature*, **353**, 737 (1991).
17. K.M. Reddy, C.V.G. Reddy and S.V. Manorama, *J. Solid State Chem*., **158**, 180 (2001).
18. B.F. Gao, Y. Ma, Y.A. Cao, J.C. Zhao and J.N. Yao, *J. Solid State Chem*., **179**, 41 (2006).
19. A. Chemseddine and T. Moritz, *Eur. J. Inorg. Chem*., 235 (1999).
20. J. Livage, M. Henry and C. Sanchez, *Prog. Solid State Chem*., **18**, 259 (1988).
21. M. Henry, J.P. Jolivet and J. Livage, *Struct. Bond., (Berlin)*, **77**, 155 (1992).
22. G.H. Wang, *J. Mol. Catal. A*, **274**, 185 (2007).
23. S.Z. Hu, A.J. Wang, X. Li and H. Löwe, *J. Phys. Chem. Solid*, **71**, 156 (2010).
24. L. Brus, *J. Phys. Chem*., **90**, 2555 (1986).
25. Z. Ding, G.Q. Lu and P.F. Greenfield, *J. Phys. Chem. B*, **104**, 4815 (2000).
26. A. Sclafani, L. Palmisano and M. Schiavello, *J. Phys. Chem*., **94**, 829 (1990).
27. A.P. Rivera, K. Tanaka, T. Hisanaga, *Appl. Catal. B*, **3**, 37 (1993).